# An Experimental Approach and a Signal Processing Method with the Common Rail Injection System of a Diesel Engine

https://doi.org/10.3991/ijoe.v17i14.27401

Thin Quynh Nguyen[1(✉)], Andrey Y. Dunin[2], Mikhail G. Shatrov[2]
[1]University of Transport and Communications, Ha Noi, Vietnam
[2]Ishlinsky Institute for Problem in Mechanics RAS, Moscow, Russia
thinquynh@utc.edu.vn

**Abstract—**This paper presents a method and results, which studies influences of the fuel flow mode on the pressure oscillation in the volumes of the accumulator fuel system. The fuel is supplied through nozzle holes into a constant volume chamber, which is installed a drain orifice for fuel discharge into the low-pressure line. Results show that the increase in the base pressure value of the fuel accumulator leads to the rise in the slope of the leading edge of the differential characteristics and the maximum dQ/dt value changes closer to the beginning moment of the fuel injection process. At the same time, the control pressure value is a significant parameter that greatly influences the shape of the injection characteristic. In addition, when using the drain orifices with different diameters, received values and differential characteristics vary during the fuel supply process. The differential characteristics of the study are the basis for implementing fuel injection control solutions.

**Keywords—**control signal, diesel engine, common rail fuel system, electrohydraulic injector, differential injection characteristic

## 1 Introduction

The diesel engine is still trusted because of its high efficiency, good economy, and large torque, so they are widely used in marine, construction, and agricultural machines, etc. [1–3]. In order to optimize the operation process for the highest efficiency, the least fuel consumption, and emission, diesel engines are getting more and more control technologies. The diesel engine control system includes intake air, fuel injection, and emission control, etc. To control those system parameters, the sensors receive the working status of the engine and send it to the ECU for processing. The ECU sends the appropriate control signal to actuators, which depends on the signal received from the sensor.

In addition, studies have demonstrated that injection pressure has a direct effect on the atomization and mixing efficiency of diesel engines [4–8]. The faster spray penetration contributes to gas utilization and increases combustion rate under high load conditions, and thereby increases engine power [9]. Along with increasing fuel injection pressure, reducing the injector hole diameter helps to reduce soot emissions [10].

In the diesel fuel system, the control process not only is the pressure, the amount of fuel per cycle, but also controls the multi-stage injection as well as with the leading edge of the injection characteristics [11,12]. Moreover, the control process is also involved in the organization and distribution of fuel in the combustion chamber of the engine [13,14]. However, the fuel injection characteristic must be determined under real conditions that develop an appropriate control strategy.

For the above purpose, this paper presents an experimental method to determine the injection characteristics of the common rail fuel system for diesel engines and a method to analyze the signal received from the experiment. The obtained results are the basis for developing a fuel system control system with ultra-high injection pressure (up to 250 MPa and more).

## 2 Experimental setup

The test is based on research, that is part of the calculation and experimental complex ICTS-MADI. The installation diagram is shown in Figure 1.

The experimental equipment includes a bed, a CR system, and a microprocessor for the controlling system, which is non-engine tests. The non-engine unit (Figure 1) has a design modular that allows it to be adapted to the fuel injection process.

To drive the high-pressure fuel pump 3, an electric motor 1 with a converter system 15 is used, which allows speed control. Pressure sensors 6 are installed in the fuel accumulator 5 of the CR system, at the inlet port of the fuel injector, and the chamber 9 for recording the injection characteristics.

During the experiment, the fuel temperature is maintained in the range of (30÷40) $^{o}$C. To maintain a constant temperature in this range, a fuel cooling system is used. The fuel temperature in tank 18 is determined through a temperature sensor 19.

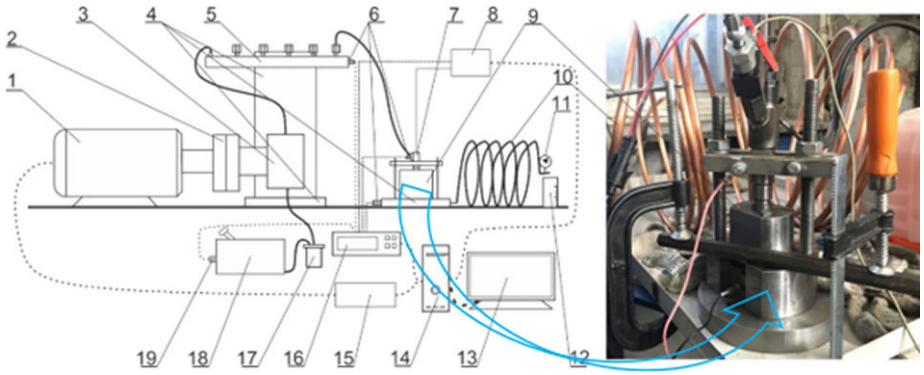


**Fig. 1.** The experimental diagram of the CR

System: 1 – Electric motor; 2 – Shaft coupling; 3 – High pressure fuel pump; 4 – Test bed of the CR system; 5 – Fuel accumulator (rail); 6 – Rail pressure sensors; 7 – Electrohydraulic injector; 8 – Converter of injector control signals; 9 – Chamber for recording injection characteristics; 10 – Low pressure fuel line; 11 – Control pressure gauge; 12 – Liquid measuring cups; 13 – Computer monitor; 14 – Computer cases;

15 – Converter for control the electric motor; 16 – Data acquisition system; 17 – Fuel filter; 18 – Fuel tank; 19 – Temperature sensor.

Table 1 shows the measurement errors of the pressures recorded during the tests.

**Table 1.** Errors of measurement pressures recorded during tests

| Measured Pressure | Error and Range of Measurement Devices |
|---|---|
| Pressure in the rail ($p_{rail}$), MPa | 0.5% of measuring range 0…400 MPa |
| Pressure at the EHI inlet port ($p_{inl}$), MPa | 0.5% of measuring range 0…400 MPa |
| Pressure in the chamber ($p_c$), MPa | 0.5% of measuring range 0…25 MPa |

The fuel system includes a high-pressure pump 3, a fuel accumulator 5, and an electrohydraulic injector (EHI) 7. The nozzle has seven holes with 0.12 mm diameter each. The EHI section is shown in Figure 2.

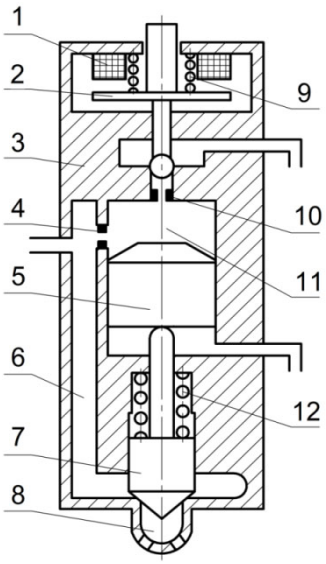


**Fig. 2.** Electrohydraulic injector

Unit: 1 – Electromagnet; 2 – Control valve; 3 – Injector body; 4 – Inlet orifice; 5 – Control piston; 6 – Control volume of the injector; 7 – Needle valve; 8 – Sack volume; 9 – Valve spring; 10 – Drain orifice; 11 – Control chamber; 12 – Nozzle spring.

As a fuel, a special calibration fluid, which is used for testing the diesel fuel system. Properties of the fluid is presented on Table 2.

**Table 2.** Physical properties of VISCOR 1487 CALBN FLUID

| Property | Value |
|---|---|
| Flash point | 75 °C |
| Ignition temperature | >200 °C |
| Density at 20 °C | 0.82 g/cm$^3$ |
| Kinematic viscosity at 40 °C | 2.4 cSt |

## 3 Results and discussion

During the research, signals from pressure sensors, which are installed in the fuel accumulator ($p_{rail}$), at the EHI inlet port ($p_{inl}$), and in the chamber ($p_c$) are recorded. At the same time, the signal from the control system to the injector solenoid valve is also written.

The experiment is carried out with a change in the duration pulse ($t_{imp}$) from 0.3 to 1.3 ms at three values of the $p_{rail\_set}$ pressure in the fuel accumulator, which is set with values of 50, 150, and 250 MPa.

The combined effect study of the $p_{rail\_set}$ and the $t_{imp}$ values is performed under the condition of a single injection.

Figure 3 shows an example of the current control signal ($U_{set}$) and a signal from sensors at the EHI inlet port ($U_{inl}$) and signal in the chamber ($U_c$).

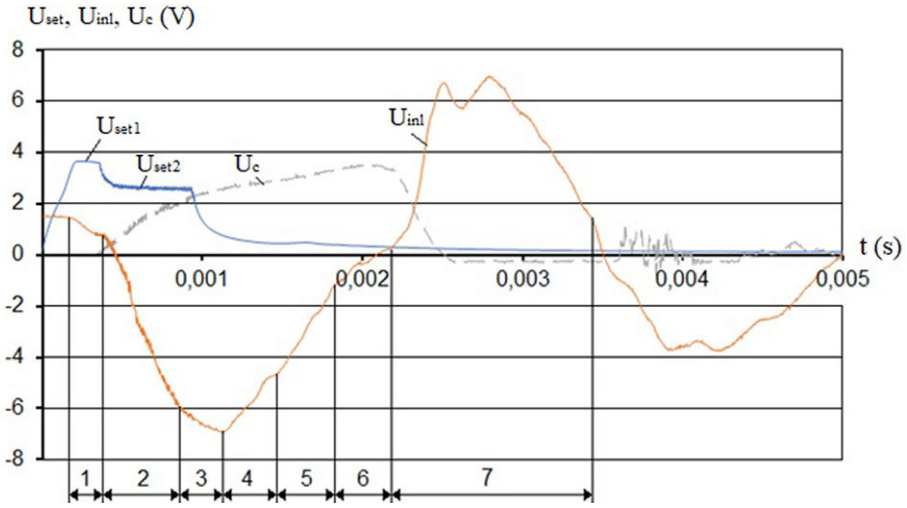


**Fig. 3.** An example of recording signals in the experiment by an electrohydraulic injector ($t_{imp}$ = 0.9 ms; $p_{rail\_set}$ = 150 MPa)

The control signal consists of the forming ($U_{set1}$), which ensures the start of the needle, and the holding parts ($U_{set2}$). Throughout all cases, the forming part is 0.3 ms. Analyzing Figure 3, seven stages (from 1 to 7) of the fuel injection process are identified:

- The first stage. This is the starting of the nozzle needle movement, which is characterized by a significant effect of the gap formed between the needle and the body nozzle. The area of the effective flow is less than that of the spray holes;
- The second stage is the move of the needle. This stage is characterized by an almost linear increase in fuel consumption with a significant drop in pressure $p_{inl}$;
- The third stage. The $p_{inl}$ value reduces with a stabilization value and it achieves the minimum value due to the movement of the nozzle needle to the maximum position ($y = y_{max}$);

- The fourth stage. In this stage, the $p_{inl}$ begins of an increase due to replenishment of fuel pressure from the fuel accumulator when the needle is at the highest position $y = y_{max}$;
- Fifth stage. The nozzle needle falls on the seat, the fuel injection through the spray holes reduces, as a result, the $p_{inl}$ value continues to rise;
- Sixth stage. The increase in speed of the $p_{inl}$ value slows down compared to stage 5. During this stage, the cross-section of the fuel flow through the gap between the needle and the nozzle body decreases with time.
- Seventh stage. At this stage, the $p_{inl}$ pressure value still increases rapidly and the pressure value appears with two characteristic peaks. The first peak is a consequence of a water hammer due to a deceleration of the fuel flow moving through the channels in the EHI, and the second is a shock when the needle closes the cone of the nozzle.

The drop in the $p_{inl}$ pressure of the first stage takes before the fuel injection start because the fuel flow from the EHI control chamber has moved when the needle valve moves. The time of stage 1 corresponds to the $U_{set1}$ part of the control signal (Figure 3). Then, the nozzle needle goes up (starting the $U_c$ signal), which is characterized by a certain delay in the $U_c$ signal.

As seen from Figure 3, in stages 2 and 3, the change in the $p_{inl}$ value is affected by the fuel outflow through the gap between the needle and the body nozzle when the $U_{set2}$ pulse of the holding part appears.

The $U_c$ signal from the sensor in the chamber illustrates the change of the $p_c$ pressure value, which positively affects by the fuel flow from the EHI nozzle holes and negatively influences by the fuel outflow from the chamber through the drain orifice. In contrast, the fuel rate through the drain orifice is influenced by the effective flow section and the $d_j$ diameter of the drain orifice. In addition, this flow rate also depends on the pressure drop between the $p_c$ values and pressure in the low-pressure line which is determined by the control valve at the end of the line (measured by the control pressure gauge 11 in Figure 1).

Figure 4 shows a comparison of the measurement results at two values of the $p_{rail\_set}$ pressure (50 and 150 MPa) with different $d_j$ values.

With an increase in the value of $d_j$ diameter, the fuel outflow rate from the chamber increases, and the $p_c$ value decreases during the injection process (comparison between Figure 4, a and Figure 4, b, between Figure 4, c and Figure 4, d). With the growth in the value of pressure in the fuel accumulator ($p_{rail\_set}$) the average rate of the fuel outflow from the spray holes increases, as a result $p_c$ value rises (comparison between Figure 4, b and Figure 4, c).

For the same modes of the EHI operation (similar $t_{imp}$ and $p_{rail\_set}$), the flow change is not observed and its value shall not exceed the error value in the measurement. The $p_{inl}$ pressure value varies with time ($p_{inl} = f(t)$). In this case, the pc value changes from 5 to 17 MPa in the main injection stage, which depends on selected $d_j$ diameter value of the drain orifice. The pc values characterize the fuel supply at the end of the compression process and operating modes of the diesel engine. Thus, the pressure value in the chamber ($p_c$) has a small effect on the fuel flow from the nozzle holes, but it is an extremely significant role in the subsequent development of the fuel spray in the cobustion chamber volume.

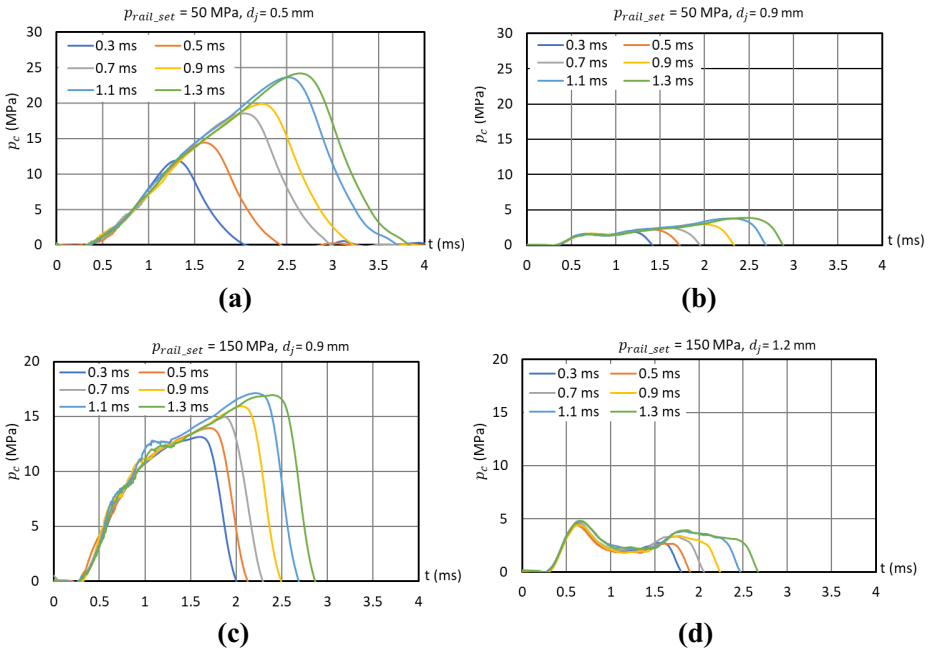


**Fig. 4.** Change in the $p_c$ pressure in the chamber depending on the drain orifice diameter

Figure 4, d shows the situation of an excessively large diameter of the drain orifice. At the beginning of injection, the fuel rate into the chamber through the nozzle holes exceeds its outflow through the drain orifice, and the $p_c$ pressure in the chamber increases quickly. Further, the $p_{inl}$ pressure decreases (stages 2 and 3 in Figure 3) because the fuel supply rate from the injector decreases and the pressure value between the chamber and the low-pressure fuel line drops, as a result, the $p_c$ pressure reduces (Figure 4, d). With an increase in the $p_{inl}$ value in stages 4 and 5 (Figure 3), the fuel rate into the chamber increases, but the outflow fuel rate through the drain orifice falls and as a consequence, an increase in the $p_c$ value is seen with 1.2 mm of the drain orifice (Figure 4, d). However, in stage 5 (Figure 3), the nozzle needle moves to the locking cone face of the nozzle body. Thus, the supply fuel amount to the spray holes reduces, and the $p_c$ value growth slows down (Figure 4, d).

The throttling of fuel in the gap between the needle and the cone face of the nozzle body in stage 6 (Figure 3) reduces, which decreases the amount of the injection fuel and as a result, the $p_c$ value decreases. After that, the injection process stops, the $p_c$ pressure value plunges and is almost linear with time ($p_c$= f(t)), which associates with the fuel flow through the drain orifice. The slope of the $p_c$ = f(t) line during this period is determined by its hydraulic characteristics.

The variation of the $p_c$ = f(t) line at $p_{rail\_set}$ = 150 MPa and the different diameters of the drain orifice is compared between Figure 4, d and 4, b. Because the fuel rate

is small, the deflection of the $p_c$ value is not observed, but there is a decrease with t = (0.7 ÷ 0.9) ms (Figure 4, b).

Comparing Figure 4, a and Figure 4, b, as well as Figure 4, c and Figure 4, d, it can see that the decrease in $p_c = f(t)$ value starts at the same point after the injection process stops at the same operating modes of the EHI ($p_{rail\_set}$, $t_{imp}$) with different $d_j$ value.

Based on the analysis of the obtained results, a method is formulated for determining the differential injection characteristic. According to this method, every moment $t$, the pressure rate in the combustion chamber ($dp_c/dt$) and the pressure rate through the drain orifice ($dp_j/dt$) is shown in formula 1:

$$\Sigma(dp/dt) = (dp_c/dt) + (dp_j/dt), \quad (1)$$

The ($dp_j/dt$) value is determined for the $p_c$ value along with the failing line $p_c = f(t)$ after the injection process stops with only fuel flow through the drain orifice which represents the hydraulic characteristic of the drain orifice. Figure 4 shows that for different $t_{imp}$ values and certain values of the $p_{rail\_set}$ and the $d_j$, the descending line parts of the $p_c = f(t)$ evenly space. In this regard, it is necessary to perform an additional registration of the $p_c = f(t)$ at the $t_{imp}$ that exceeds the maximum value of control duration pulse when the injection characteristics in the change range of the $t_{imp}$ value are performed.

When the method is implemented for determining the differential injection characteristics through the formula $\Sigma(dp/dt) = f(t)$, it is necessary to select the $d_j$ diameter value, which ensures a monotonous increase in the $p_c$ pressure (except for the end of stage 6, Figure 3) during the injection process, as shown in Figure 4, a and Figure 4, c.

The conversion $\Sigma(dp/dt) = f(t)$ in the differential characteristics of the injection $dQ/dt = f(t)$ is made through a coefficient which represents through a ratio between the area limited $\Sigma(dp/dt) = f(t)$ and the amount of injection cycle ($Q_c$) in the fuel injection cases ($p_{rail\_set}$, $t_{imp}$) (Figure 5).

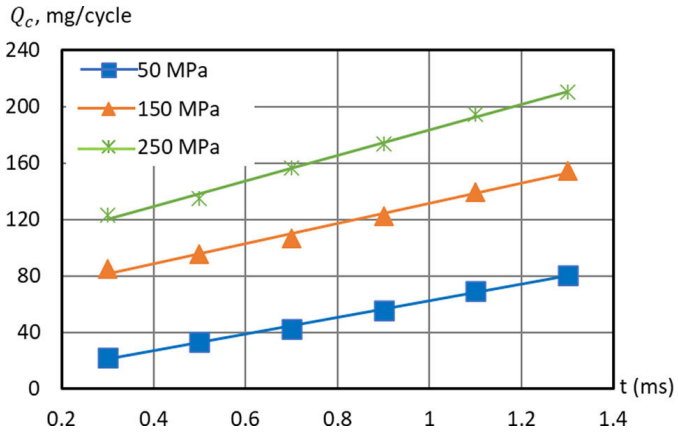


**Fig. 5.** Change of the cycle fuel supply ($Q_c$) depends on the $p_{rail\_set}$ pressure value in the fuel accumulator and the duration of the control pulse ($t_{imp}$)

Figure 6 shows $p_{inl}$ = f(t) in the fuel injection process, which depends on the duration $t_{imp}$ of the control pulse.

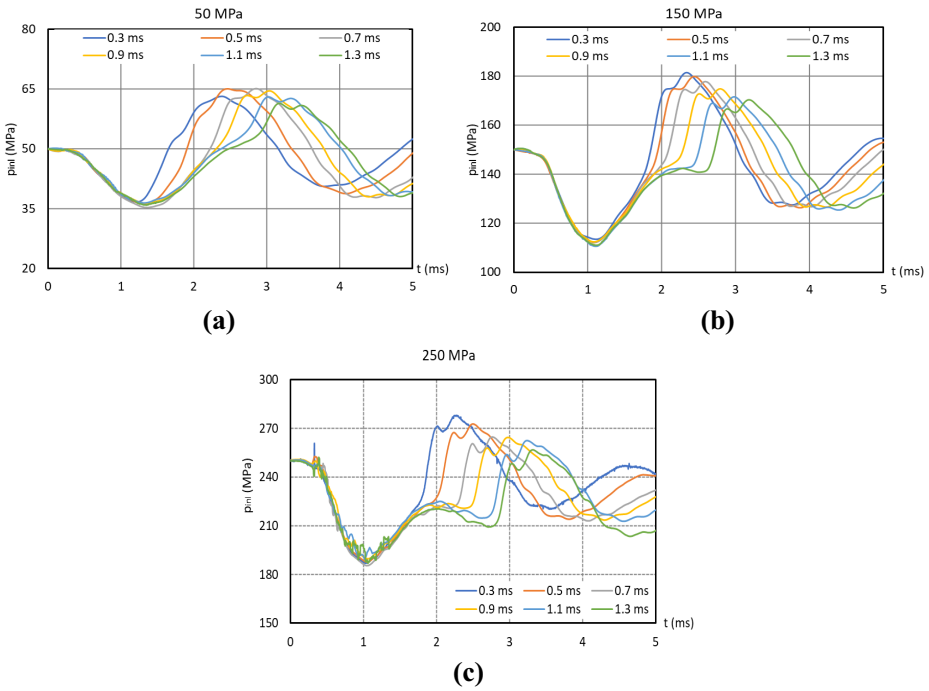


**Fig. 6.** Influence of the $p_{rail\_set}$ pressure value in the fuel accumulator and the duration of the $t_{imp}$ control pulse on the $p_{inl}$ pressure value at the injector inlet port: **(a)** 50 MPa; **(b)** 150 MPa; **(c)** 250 MPa

In this case, Figure 7 illustrates the comparison between the pressure change at the injector inlet port ($\Delta p_{inl}$) with different $p_{rail\_set}$ values and three $t_{imp}$ values 0.3, 0.7, and 1.3 ms.

With an increase in the $p_{rail\_set}$ the fuel flow rate through the spray holes goes up, which leads to a drop in the $p_{inl}$ value with a greater $\Delta p_{inl}$ value at stage 2 of the injection process when the needle is lifted (Figure 7). At the same time, the higher values of the fuel flow rate and the $p_{inl}$ value are (Figure 6), the bigger the fuel flow rate gets. This leads to an increase in the $Q_c$ value at the same $t_{imp}$ value.

When the fuel supply rises with a growth in the $p_{rail\_set}$, the $\Delta p_{inl}$ value drop in the next stages (3÷6) of the injection processes also goes up (Figure 7).

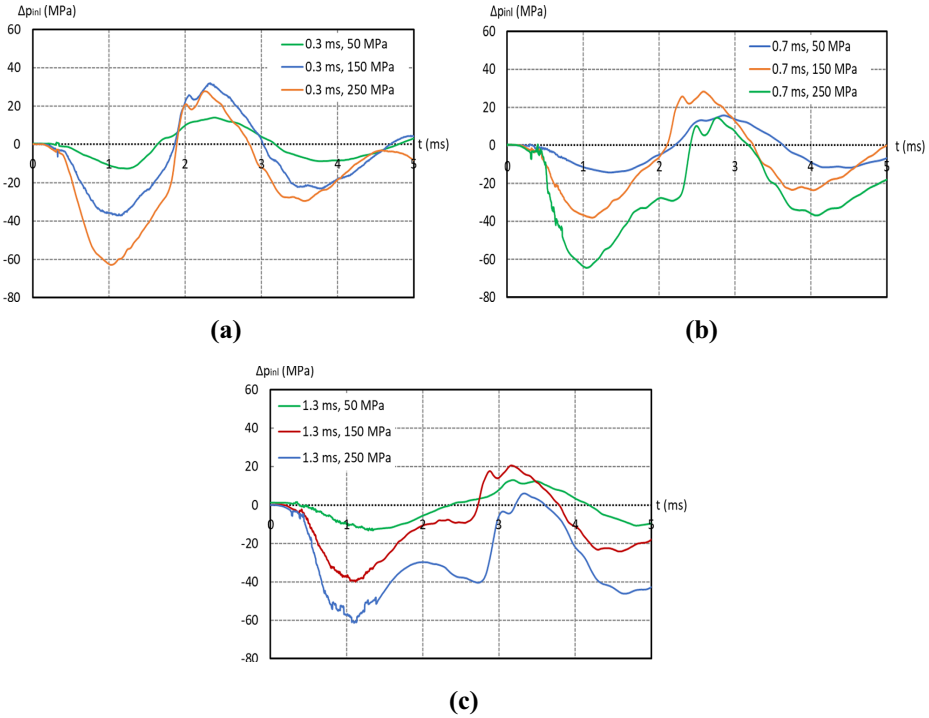


**Fig. 7.** Influence of the $p_{rail\_set}$ pressure value in the fuel accumulator and the duration of the $t_{imp}$ control pulse on the pressure change ($\Delta p_{inl}$) at the injector inlet port: **(a)** $t_{imp}$ = 0.3 ms; **(b)** $t_{imp}$ = 0.7 ms; **(c)** $t_{imp}$ = 1.3 ms

An increase in the fuel flow rate with a rise in the $p_{rail\_set}$ leads to the release of more energy when it is decelerated (water hammer). The result is a growth in the $p_{inl}$ value of the first peak in stage 7 (Figure 7). In this case, because the absolute value $p_{inl}$ at the end of the control duration pulse is big and the EHI valve is closed, therefore the fuel filling rate in the control chamber of the nozzle is fast, as a consequence, the fall speed of the needle on the seat increases. The energy in the fall process of the needle rises, which is shown an increase in the $p_{inl}$ value of the second peak at stage 7 (Figure 7). This is especially noticed with a rise in the $t_{imp}$ (Figure 7, c).

Besides the intensity of the fuel flow through the nozzle holes, the $p_{inl}$ value is affected by the fuel outflow from the EHI control chamber when the valve opens. The early termination of the control pulse (the decrease in the $t_{imp}$) contributes to a decrease in the $p_{inl}$ drop rate, but this effect is hardly noticeable because the effective flow section of the nozzle is larger than the flow through the gap between the needle and nozzle body. However, the lower the $t_{imp}$ value and the higher the $p_{inl}$ pressure are, the higher the filling rate in the control chamber gets and also the higher the needle speed falls on the seat. This is accompanied by a growth in the value of the second $p_{inl}$ peak in stage 7 (Figure 6, b and Figure 6, c). The high needle falling speed on the seat causes a rise in flow deceleration and an increase in the $p_{inl}$ value of the first peak in stage 7 (Figure 6, b and Figure 6, c). In this case, an increase in the $t_{imp}$ value contributes to a rise in the deflection of the $p_{inl}$ pressure value between the two peaks in stage 7 (Figure 6).

The relationship between the decrease in the $t_{imp}$ value and the increase in the falling speed of the needle on the seat is influenced by the $p_{rail\_set}$ value. Growth in the $p_{rail\_set}$ value contributes to a drop in the $p_{inl}$ in stage 2 of the injection process. This is clearly seen from the comparison of Figure 6, a ($p_{rail\_set}$ = 50 MPa) with Figure 6, b ($p_{rail\_set}$ = 150 MPa) and Figure 6, c ($p_{rail\_set}$ = 250 MPa). At $p_{rail\_set}$ = 50 MPa and $t_{imp}$ = 0.3 ms, the $p_{inl}$ value of the pressure peaks in stage 7 are even lower than it at $t_{imp}$ = 0.5 ms.

The results of the received signals processing from the sensors with the formula $p_{inl}$ = f(t) and mass flow rate d$Q$/dt = f(t) and the control pulse at the $p_{rail\_set}$ values equal to 50, 150, and 250 MPa are shown in Figure 8, Figure 9 and Figure 10, respectively.

The increase in the $p_{rail\_set}$ value and its effect on the $p_{inl}$ change is described above, which leads to a rise in the slope of the leading edge of the differential injection characteristic and the maximum d$Q$/dt changes closer to the beginning of the fuel injection (Figure 8, Figure 9 and Figure 10). This problem is explained by the decrease in the intensity of fuel supply which is represented by the fall in the $p_{inl}$ value. The middle and at the end of the fuel injection process are affected by the change in the $p_{inl}$ value in stages (4 ÷ 6).

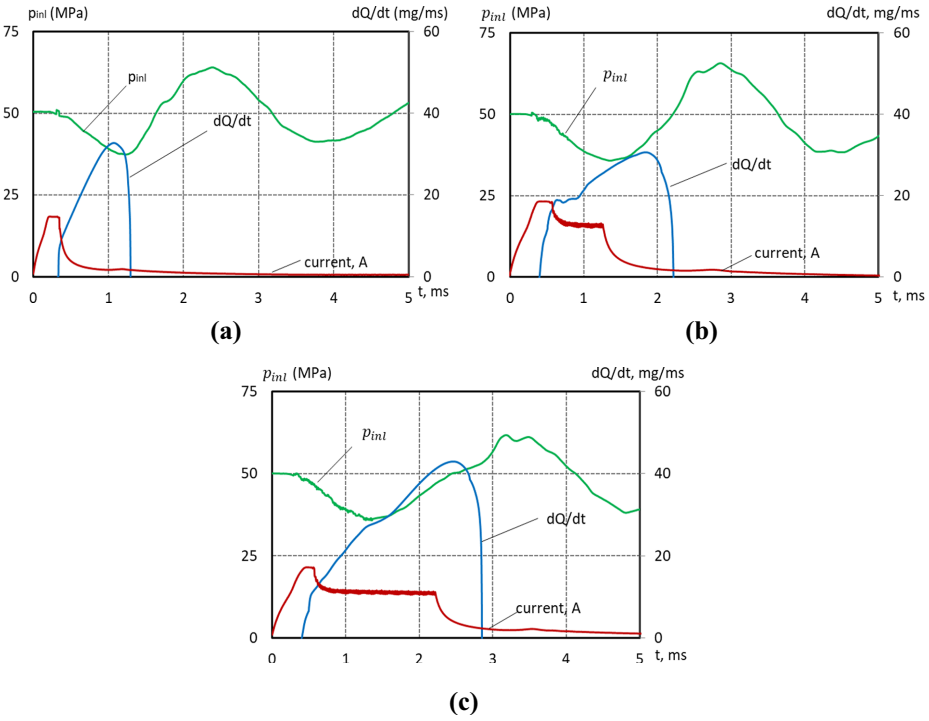


**Fig. 8.** The $p_{inl}$ pressure at the injector inlet port and differential injection characteristic d$Q$/dt ($p_{rail\_set}$ = 50 MPa): **(a)** $t_{imp}$ = 0.3 ms; **(b)** $t_{imp}$ = 0.7 ms; **(c)** $t_{imp}$ = 1.3 ms

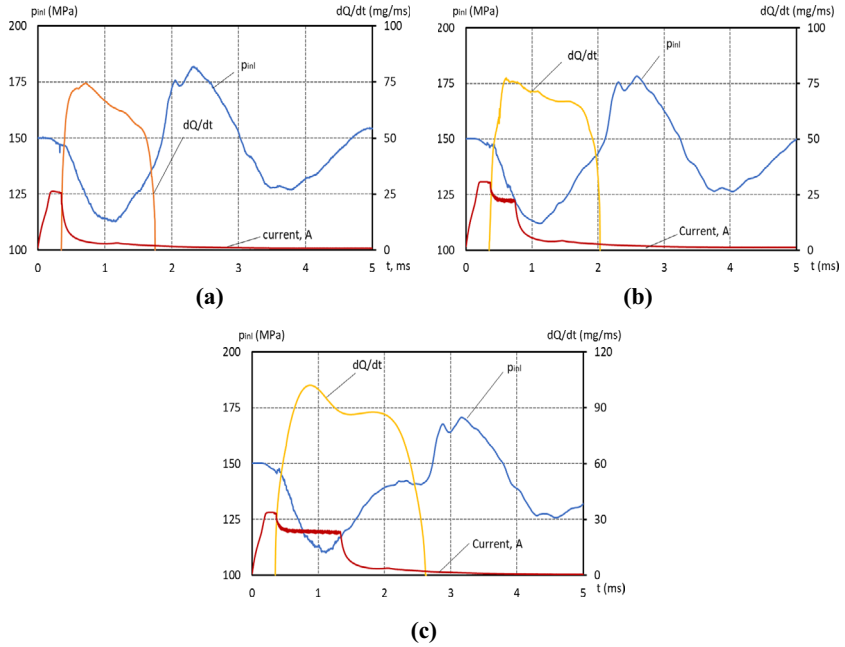


**Fig. 9.** The $p_{inl}$ pressure at the injector inlet port and differential injection characteristic d$Q$/dt ($p_{rail\_set}$ = 150 MPa): **(a)** $t_{imp}$ = 0.3 ms; **(b)** $t_{imp}$ = 0.7 ms; **(c)** $t_{imp}$ = 1.3 ms

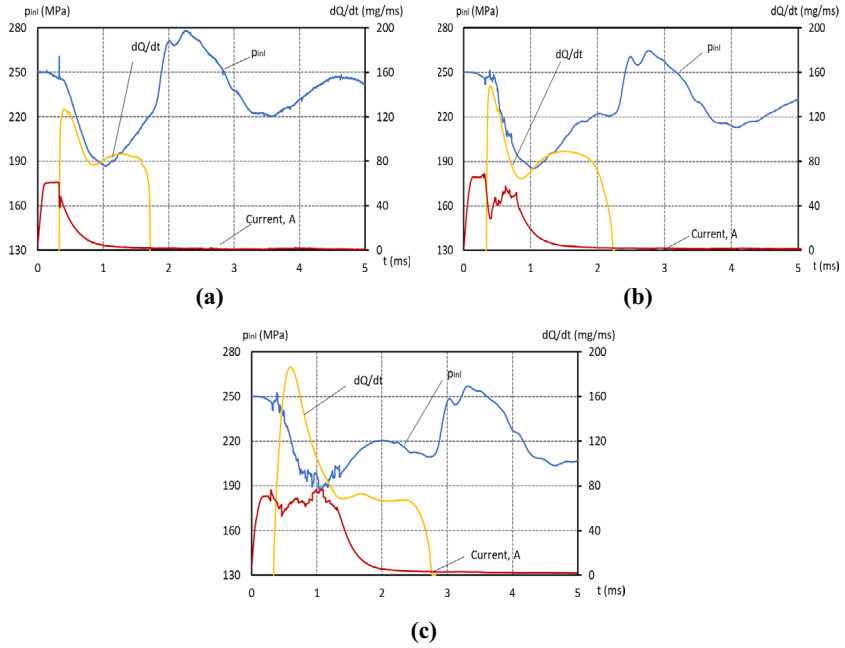


**Fig. 10.** The $p_{inl}$ pressure at the injector inlet port and differential injection characteristic d$Q$/dt ($p_{rail\_set}$ = 250 MPa): **(a)** $t_{imp}$ = 0.3 ms; **(b)** $t_{imp}$ = 0.7 ms; **(c)** $t_{imp}$ = 1.3 ms

With an increase in the $p_{rail\_set}$ value, more fuel is injected at the moment of falling rate (comparison of Figure 8 with Figure 9 and Figure 10). In this case, the higher the $p_{rail\_set}$ amount is, the bigger the intensity value of the d$Q$/dt drops from the maximum value to the end of injection (comparison of Figure 9 and 10). Thus, the $p_{rail\_set}$ control value is a significant parameter which influences the shape of the injection characteristic. It also redistributes the fuel amount which is supplied by the fuel injection process by changing the injection duration.

It is obvious that the studied effects on the $p_{inl}$ change (Figure 6 and Figure 7) have a combined effect on the $p_{rail\_set}$, $t_{imp}$, the speed of the control valve, the volume of the control chamber, the effective flow section of the nozzle, and the internal volume in the EHI body and the move of the nozzle needle to the cone face.

## 4 Conclusion

Qualitative and quantitative analysis of the research results suggests the conclusions that a method is developed to determine the differential characteristics of the fuel injection by summing at each moment $t$ with the change rate of pressure in the chamber (d$p_c$/dt) and the fall rate of pressure due to the fuel outflow through the drain orifice (d$p_j$/dt). The increase in the base pressure value of the $p_{rail\_set}$ fuel accumulator leads to the rise in the slope of the leading edge of the differential characteristics and the maximum d$Q$/dt value changes closer to the beginning moment of the fuel injection process. The $p_{rail\_set}$ control value is a significant parameter that influences the shape of the injection characteristic. It also redistributes the fuel amount which is supplied by the fuel injection process between the starting and the final stages with changing of the injection duration.

## 5 Acknowledgements

This work was supported by the Russian Science Foundation [grant number 19-19-00598]. Site: https://www.rscf.ru/

## 6 References

[1] Kim, J., Kakami, S., Jin, Y., Nishida, K., and Ogata, Y. (2019). Internal Fuel Flow, Near-Field and Far-Field Spray Evolution, and Mixture Formation Characteristics of Diesel Injectors-A Comparison between Multi-and Single-Hole Injectors (No. 2019-01-0273). SAE Technical Paper. https://doi.org/10.4271/2019-01-0273

[2] Dunin, A. Y., Quynh, N. T., Shatrov, M. G., and Golubkov, L. N. (2020). Analysis of the nozzle hole diameter effect to common rail diesel engine characteristics using a calculated model of an internal combustion engine. International Journal of Emerging Trends in Engineering Research, 8: 2301–2308. https://doi.org/10.30534/ijeter/2020/17862020

[3] Quynh, N. T., Dunin, A. Y., Duc, L. H., and Shatrov, M. G. (2021). Engine performance, emissions characteristics of the compression ignition engine using HHO gas (Brown's gas). IOP Conference Series: Materials Science and Engineering, 1159: 012-055. https://doi.org/10.1088/1757-899X/1159/1/012055

[4] Wang, Y., Yu, Y., Li, G., and Jia, T. Experimental investigation on the characteristics of supersonic fuel spray and configurations of induced shock waves. Scientific Reports,7. https://doi.org/10.1038/srep39685
[5] Mohan, B., Yang, W., and Chou S Kiang. (2013). Fuel injection strategies for performance improvement and emissions reduction in compression ignition engines—A review. Renewable and Sustainable Energy Reviews, 28: 10–16. https://doi.org/10.1016/j.rser.2013.08.051
[6] Dimitriou, P., Wang, W., and Peng, Z. (2015). A piston geometry and nozzle spray angle investigation in a DI diesel engine by quantifying the air-fuel mixture. International Journal of Spray and Combustion Dynamics, 7: 1–24. https://doi.org/10.1260/1756-8277.7.1.1
[7] Keum, S., Pal, P., Im, H. G., Babajimopoulos, A., and Assanis, D. N. (2016). Effects of fuel injection parameters on the performance of homogeneous charge compression ignition at low-load conditions. International Journal of Engine Research, 17: 413–420. https://doi.org/10.1177/1468087415583597
[8] Agarwal, A. K., Srivastava, D. K., Dhar, A., Maurya, R. K., Shukla, P. C., and Singh, A. P. (2013). Effect of fuel injection timing and pressure on combustion, emissions and performance characteristics of a single cylinder diesel engine. Fuel, 111: 374–383. https://doi.org/10.1016/j.fuel.2013.03.016
[9] Tao, F., and Bergstrand, P. (2008). Effect of ultra-high injection pressure on diesel ignition and flame under high-boost conditions. SAE Technical Paper. https://doi.org/10.4271/2008-01-1603
[10] Wang, X., Huang, Z., Zhang, W., Kuti, O. A., and Nishida, K. (2011). Effects of ultra-high injection pressure and micro-hole nozzle on flame structure and soot formation of impinging diesel spray. Applied Energy, 88: 1620–1628. https://doi.org/10.1016/j.apenergy.2010.11.035
[11] Dunin, A. Y., Shatrov, M. G., Golubkov, L. N., and Yakovenko, A. L. (2020). Providing Boot-Type Injection Rate Shape by Electric Impulse Control of the Common Rail Injector. Proceedings of Higher Educational Institutions Machine Building. 1: 32–42. https://doi.org/10.18698/0536-1044-2020-1-32-42
[12] Shatrov, M. G., Malchuk, V. I., Dunin, A. U., and Yakovenko, A. L. (2016). The influence of location of input edges of injection holes on hydraulic characteristics of injector the diesel fuel system. International Journal of Applied Engineering Research, 11: 10267–10273.
[13] Dunin, A., Shatrov, M., Malchuk, V., Skorodelov, S., Sinyavski, V., and Yakovenko, A. (2019). Simulation of fuel injection through a nozzle having different position of the spray holes. Periodicals of Engineering and Natural Sciences (PEN), 7: 458–464. https://doi.org/10.21533/pen.v7i1.403
[14] Iakovenko, A., Dunin, A., Dushkin, P., Savastenko, E., and Shatrov, M. (2019). The influence of mass composition of water-fuel emulsion on ecological characteristics of a diesel engine. Energies, 12: 2689. https://doi.org/10.3390/en12142689

## 7 Authors

**Thin Quynh Nguyen,** Faculty of Mechanical Engineering, University of Transport and Communications, Ha Noi, 100000, Vietnam.

**Andrey Y. Dunin,** Ishlinsky Institute for Problem in Mechanics RAS, 101-1, Vernadskogo Prosp., Moscow, 119526, Russia. E-mail: a.u.dunin@yandex.ru

**Mikhail G. Shatrov,** Ishlinsky Institute for Problem in Mechanics RAS, 101-1, Vernadskogo Prosp., Moscow, 119526, Russia. E-mail: dvs@madi.ru

Article submitted 2021-09-07. Resubmitted 2021-10-13. Final acceptance 2021-10-13. Final version published as submitted by the authors.